Citation: Fangzhen Liu, Luhua Liu, Chao Ou. Chaotification method for the glide midcourse trajectory. *Journal of Harbin Institute of Technology(New Series)*. DOI:10.11916/j.issn.1005-9113.2024029.

Chaotification Method for the Glide Midcourse Trajectory

Fangzhen Liu[1,2], Luhua Liu[1,2] and Chao Ou[3,4]**

(*1.School of Aeronautics and Astronautics, Sun Yat-Sen University, Shenzhen 518107, China;*
2.Shenzhen Key Laboratory of Intelligent Microsatellite Constellation, Shenzhen 518107, China;
3.School of Aeronautics and Astronautics, Huazhong University of Science and Technology, Wuhan 430074, China;
4.China Aerodynamics Research and Development Center, Mianyang 621000, China)

Abstract: In order to enhance the penetration performance of hypersonic gliding vehicle, a chaotification method of gliding midcourse based on flight dynamics is proposed. Firstly, a chaotic series-based angle of attack (AOA) control algorithm and an AOA switching control algorithm considering flight altitude are proposed in this study based on a simple chaotic system with considerations of AOA constraints and process constraints. Secondly, the Lyapunov exponent algorithm of continuous system is applied to verify the chaotic characteristic of flight trajectories. Thirdly, a stability region analysis method is proposed based on a conservative dynamics, which can be applied to the stability region analysis of general complex dynamics. Finally, the simulations show that both control algorithms can realize the chaotification of trajectories, and the flight trajectories obtained by the AOA switching control algorithm are feasible.

Keywords: Maneuver; Chaotification; Lyapunov exponent

CLC number: V412.4 **Document code**: A **Article ID**: 1005-9113(2024)00-0000-12

0 Introduction

If Hypersonic Glider Vehicles (HGVs)[1-3] need to pass through no-fly zones that cannot be bypassed, it is necessary to improve the capability of penetration to cross these no-fly zones safely, it is of great significance for achieving the globally accessible goals.

Reentry trajectories of HGVs generally have two forms: Equilibrium glide and jumping glide. The trajectories change with the reentry attitude, thus HGVs have a certain capability of penetration. However, trajectory prediction methods based on characteristic function[4] and maneuver mode on-line identification[5] in specific situations can achieve high-precision prediction of flight trajectories. To address the challenges of increasingly intelligent defense systems, maneuvering control strategies can be used to improve the penetration performance of vehicles, such as sine maneuvering mode[6], Pendulum maneuvering mode[7] and spiral maneuver mode[8]. However, the flight trajectories with these maneuver modes are highly regular. Hu et al.[9] employed probabilistic-based intention inference for long-term trajectory prediction, and employed maneuver mode online identification methods to achieve high-precision short-term trajectory prediction. According to the experimental results, the flight trajectory can be accurately predicted under the fixed maneuvering mode. This means an increase in the probability of being intercepted.

In order to reduce the probability of interception and improve the penetration performance, researchers focus on the penetration trajectory optimization. Yan et al.[10] formulated a complex nonconvex penetration problem as a sequence of easily solved second-order cone programming problem. The proposed strategy has a considerable miss distance and is computationally efficient. Shen et al.[11-12] investigated the problem of HGV encountering two interceptors by formulating a nonconvex optimal control problem as a second-order cone programming problem. The simulations illustrate that the method can effectively improve the penetration capability of vehicles. The data set was constructed using second-order cone programming

Received 2024-03-17.
Sponsored by the National Natural Science Foundation of China (Grant No. 61973326), the Shenzhen Science and Technology Program (Grant No. ZDSYS20210623091808026), and the Key Laboratory of Cross-Domain Flight Interdisciplinary Technology (Grant No.2024-KF02201).
* Corresponding author. Luhua Liu, Ph.D., Professor. E-mail: flightdc@mail.sysu.edu.cn;Chao Ou,Ph.D Candidate,Senior Engineer,ouchao_jg@126.com.

problem with different initial states, and the deep neural network was trained offline to be used as a controller. The real-time performance and effectiveness of the scheme were verified by Monte Carlo tests.

In addition, it is also an effective method to enhance the penetration capability of vehicles by improving the unpredictability of trajectories through chaotification. The main characteristic of chaotic trajectories is that tiny perturbations in the initial state—such as initial velocity, altitude, and flight path angle—will have wide effects on the trajectories, which can enhance the unpredictability of the flight trajectories.

Sun et al.[13] controlled the rudder angle for maneuver guidance, and the command was based on a chaotic series generated by a state variable of Rossler system, which made the flight trajectories chaotic. This indicates that the chaotification of flight trajectory through control is feasible, but due to the limited control capability, the change of trajectories is small, and the enhancement of penetration capability is weak. Therefore, the purpose of this study is not only to make the flight trajectories chaotic, but also to make a significant difference between chaotic trajectories in order to improve vehicles' penetration capability. Chaotic systems are well known for their high sensitivity to the initial state, a property that is detrimental in fields such as satellite attitude control[14], satellite orbit maintenance[15], and gear motion[16], the property needs to be inhibited by control design. On the contrary, it is beneficial in the fields of confidential communication and material mixing, which can improve the security of information transmission[17-21], and improve the mixing efficiency of nanomaterials[22].

Wang et al.[23] studied various types of equilibria, symmetry, conservativity, multi-stability, hidden and multi-scroll attractors based on low-dimensional simple chaotic systems, demonstrating the complex characteristics of simple chaotic systems and the potential of engineering utilization. Wang et al.[24] applied a systematic operation of complex number to generate multi-folded motion trajectories. Their results illustrate that simple systems can achieve the desired chaotic characteristic by control design. Meanwhile, the study on orbital chaotic dynamics by Das and Roychowdhury[25] and the further study on multiple forms of chaotic attractors by Li et al.[26] proved that the effects of system parameters on chaotic characteristic are significant. Therefore, the selection and design of each parameter in the process of chaotification need to be discussed and studied in detail.

Different from the traditional design concept of penetration trajectory, inspired by the strong unpredictability of chaotic system state trajectory, this paper expects to strengthen the unpredictability of flight trajectory through chaotification of flight dynamics system, so as to improve the penetration capability of HGVs. In this study, a simple low-dimensional chaotic system is combined, and trajectory chaotification controllers based on state feedback are designed considering AOA constraints and process constraints. Importantly, the method does not require the specification of penetration trajectories for the control method design, but rather improves the unpredictability of the trajectory through the chaotification of dynamics. Finally, applying the Lyapunov exponent to verify the chaotic characteristic of flight trajectories, and analyze the stability region by a conservative dynamics, which verify the feasibility and effectiveness of the trajectory chaotification methods proposed in this paper. Meanwhile, the stability region analysis method proposed in this paper is of practical engineering value in the work of analyzing the stability region of general complex systems.

1 Hypersonic Gliding Vehicle Model

Since the earth rotation and oblateness have little effect on trajectory characteristics during maneuvering flight, suppose the earth is a sphere with uniform mass, and the rotation of the earth is ignored. Without loss of generality, a feasibility study of chaotification methods can be carried out in the longitudinal channel.

1.1 Aerodynamic Model

In this study, the aerodynamic coefficients are formulated as polynomial functions of attack angle α and flight Mach number Ma. The lift coefficient $C_l(\alpha, \mathrm{Ma})$ and drag coefficient $C_d(\alpha, \mathrm{Ma})$ models were established. The force model of vehicles can be expressed as follows:

$$\begin{cases} L = C_l q S_{\mathrm{ref}} \\ D = C_d q S_{\mathrm{ref}} \end{cases}$$

where, L and D are lift and drag; q and S_{ref} are flight aerodynamic pressure and reference aerodynamic area.

The atmospheric model applies the US Standard Atmosphere model (USSA76).

1.2 Kinetic Model

Based on the aerodynamic model, the motion model[27] of the vehicle mass center in the longitudinal channel can be simplified as:

$$\begin{cases} \dot{V} = -\dfrac{D}{m} - \dfrac{\mu}{(R_0+h)^2}\sin(\Theta) \\ \dot{\Theta} = \dfrac{L}{mV} + \dfrac{V}{R_0+h}\cos(\Theta) - \dfrac{\mu}{(R_0+h)^2 V}\cos(\Theta) \\ \dot{h} = V\sin(\Theta) \\ \dot{L} = \dfrac{R_0 V\cos(\Theta)}{R_0+h} \end{cases} \tag{1}$$

where R_0 and μ are average radius of the earth and the gravitational constant; V, Θ, h, L and m are velocity, flight path angle, altitude and mass, respectively.

The design process of trajectory chaotification controllers is described in detail subsequently.

2 Trajectory Chaotification Method Based on AOA Design

In order to achieve chaotic and feasible penetration trajectories, a control design for the AOA command is required. The chaotic characteristics of systems can be expressed by Lyapunov exponent. While the chaotic flight dynamics is complex and it is difficult to theoretically analyze its stability region. This paper will analyze the stability region of chaotic trajectories based on conservative dynamics.

2.1 Chaos Analysis Theory

An important characteristic of chaotic systems is high sensitivity to initial state, which can be expressed by the Lyapunov exponent, the definition of that is as follows. Two initial state points, with distance C from each other and whose average distance varies with time[13], can be expressed as:

$$d(t) = Ce^{\lambda t}$$

where λ denotes the Lyapunov exponent. The average separation distance increases exponentially when λ is more than 0, indicating that the system is chaotic. Taking the Rossler system as an example, the Lyapunov exponent algorithm for continuous systems was introduced. The dynamics equation of Rossler system is:

$$\begin{cases} \dot{x} = k_{\text{Rossler}}(-y-z) \\ \dot{y} = k_{\text{Rossler}}(x + R_a \times y) \\ \dot{z} = k_{\text{Rossler}}[R_b + z(x - R_c)] \end{cases} \tag{2}$$

where x, y and z are state variables; k_{Rossler} is a scaling factor, which can regulate the change frequency of the state variables; R_a, R_b and R_c are system variables, which have significant effects on chaotic behavior of the system.

The phase portrait (f,g,h) of the Rossler system can be obtained by solving Eq. (2) based on an initial state (x_0,y_0,z_0). N reference points are uniformly selected on the phase portrait (x_k,y_k,z_k) for $k=1,2,\cdots,N$.

The interval between the initial state point and each reference point is Δt, then Jacobi Matrix $\boldsymbol{J}_k^{(\Delta t)}$ at the kth reference point is:

$$\boldsymbol{J}_k^{(\Delta t)} = \left[\begin{matrix} \left.\dfrac{\partial f}{\partial x}\right|_{\Delta t} & \left.\dfrac{\partial f}{\partial y}\right|_{\Delta t} & \left.\dfrac{\partial f}{\partial z}\right|_{\Delta t} \\ \left.\dfrac{\partial g}{\partial x}\right|_{\Delta t} & \left.\dfrac{\partial g}{\partial y}\right|_{\Delta t} & \left.\dfrac{\partial g}{\partial z}\right|_{\Delta t} \\ \left.\dfrac{\partial h}{\partial x}\right|_{\Delta t} & \left.\dfrac{\partial h}{\partial y}\right|_{\Delta t} & \left.\dfrac{\partial h}{\partial z}\right|_{\Delta t} \end{matrix}\right]\Bigg|_{(x_k,y_k,z_k)}$$

Taking $\boldsymbol{J}_0^{(\Delta t)}$ as a square matrix of order 3 with all elements being 1. $\boldsymbol{J}^{(\Delta t)}$ is expressed as:

$$\boldsymbol{J}^{(\Delta t)} = \prod_{k=0}^{N} \boldsymbol{J}_k^{(\Delta t)}$$

The Lyapunov exponent for the intervals $\lambda^{(\Delta t)}$ is obtained by taking the natural logarithm of the largest eigenvalue of the matrix $\boldsymbol{J}^{(\Delta t)}$ and dividing by N:

$$\lambda^{(\Delta t)} = \frac{\ln\{\max[\text{eig}(\boldsymbol{J}^{(\Delta t)})]\}}{N}$$

The system is chaotic when the Lyapunov exponent is more than zero.

2.2 Stability Region Analysis Theory Based on Conservative System

The ideal penetration trajectory requires flying towards the target, better maneuverability, and longer range, which raises requirements for flight path angle and altitude. Under the condition of Mach number 15 and angle of attack 10°, the requirements are: 1) The normal overload is more than 0.33; 2) The axial acceleration load is less than 4; 3) The velocity component in altitude direction is less than 450 m/s. Then the required stability region of flight state is:

$$\Theta \in [-5.72°, 5.73°], h \in [35\ \text{km}, 52\ \text{km}] \tag{3}$$

According to the definition of Lyapunov stable[28], if phase portraits start from a spherical

domain $S(\delta)$ of an equilibrium point x_e, and does not beyond a spherical domain $S(\varepsilon)$ at any time thereafter, the equilibrium state x_e is called Lyapunov stable. Obviously, the equilibrium glide state is the equilibrium point of the system. But the flight dynamics system is a typical dissipative one, in which mechanical energy gradually decreases until landing, and the equilibrium point constantly changes. In order to maintain the equilibrium point, the dissipative term in the dynamics is ignored, then the conservative dynamics is constructed as follows:

$$\begin{cases} \dot{V} = -\dfrac{\mu}{(R_0+h)^2}\sin(\Theta) \\ \dot{\Theta} = \dfrac{L}{mV} + \dfrac{V}{R_0+h}\cos(\Theta) - \dfrac{\mu}{(R_0+h)^2 V}\cos(\Theta) \\ \dot{h} = V\sin(\Theta) \\ \dot{L} = \dfrac{R_0 V\cos(\Theta)}{R_0+h} \end{cases} \tag{4}$$

The system mechanical energy is constant, and the change of altitude only has tiny effect on velocity. Therefore, the velocity can be regarded as constant, then the equilibrium glide state is constant, namely that the equilibrium point does not change, so it is feasible to analyze the stability region at the equilibrium point. The phase portrait starts from the initial state point, and when the simulation time is long enough, the feasibility of trajectories can be analyzed by the upper and lower bounds of the stability region at the equilibrium point, which can be approximated by the maximum and minimum values of state time series.

2.3 Design of Chaotic Series-based AOA Control Method

The state variable x in Eq. (2) changes continuously and slowly, and chaotic trajectories can be realized by applying x to the control design[13]. Taking the vehicle attitude control response characteristics into account, the range of AOA and its change rate are limited to:

$$\alpha_{(t)} \in [5°, 30°], \quad \dot{\alpha}_{(t)} \in [-3°/s, 3°/s] \tag{5}$$

Taking the AOA command as the sum of x and the maximum lift-to-drag ratio AOA α^*:

$$\alpha_{\mathrm{cmd}}(t) = x^{\mathrm{Rossler}}(t) + \alpha^* \tag{6}$$

The flight simulation flow chart is shown as the dotted line in Fig. 1. The input is the initial state of vehicles x_0^{Flight}; firstly, the initial state of Rossler system x_0^{Rossler} is obtained by Eq. (7); secondly, the state of Rossler system x^{Rossler} is obtained by solving the dynamical equation (Eq. (2)); thirdly, the AOA command is obtained by Eq. (6); then, the actual AOA can be obtained by applying the constraints given in Eq. (5); finally, the flight state x^{Flight} is obtained by solving the dynamics equation (Eq. (1)).

The larger the k_{Rossler}, the higher the change frequency of x. Applying chaotic state x time series with different change frequencies to AOA control will result in different flight trajectories. However, there are two disadvantages of this control method:

1) The change frequency of chaotic state x time series is beyond the AOA constraints specified in Eq. (5);

2) High impacts on range and maneuverability.

Further improvement of the control method for flight trajectory chaotification is needed.

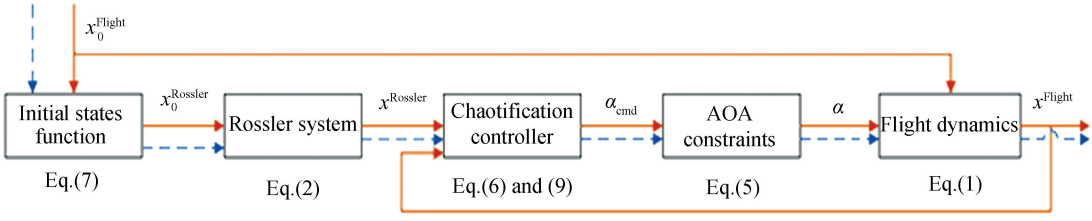

Fig.1 Flight simulation flow chart

2.4 Design of AOA Switching Control Method Considering Flight Altitude

Due to the fact that the maneuverability of vehicles is weak at high altitude and the aerodynamic drag is high at low altitude, the effects of altitude on flight state need to be taken into account. An efficient maneuvering altitude range is defined as $[H_1, H_2]$, within which vehicles are maneuverable and have low aerodynamic drag. In addition, high flight path angle is harmful to maneuvering flight, so it is also necessary to consider the range of flight path angle in the control design.

1) When the flight altitude is higher than H_2, the vehicle should enter the altitude range $[H_1, H_2]$ with low flight path angle, so it needs to maintain high AOA, as shown in region ① of Fig.2, and the color gradation of the data points indicates the size of AOA command;

2) In the altitude range $[H_1, H_2]$, the aerodynamic drag has a low impact on the range, vehicles can perform maneuvering flight refer to AOA commands continuously, as shown in the region ② of Fig.2;

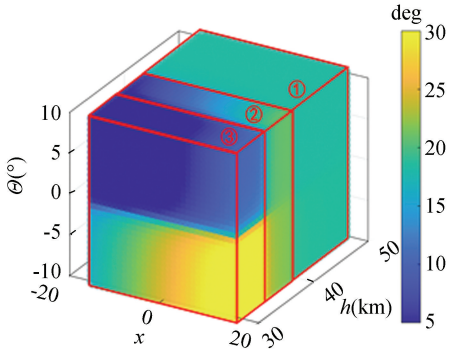

Fig. 2 Requirements for AOA switching control considering flight altitude

3) When the flight altitude is less than H_1, it is necessary to raise AOA to increase the lift and avoid altitude being too low according to the flight path angle, as shown in region ③ of Fig.2.

The color of each scatter point in Fig.2 corresponds to the number on the color scale, namely, the angle of attack α. Additionally, x is the state variable of the Rossler system, h is the flight altitude, and Θ is the flight path angle.

3 Parameters Selection

3.1 Parameters Selection of Rossler System

The initial state of Rossler system is an important parameter. Considering that the main feature of a chaotic system is that the disturbances in initial state will greatly affect the state trajectory, it is necessary to analyze the feasibility of initial state. The effect of the initial state on x state time series is shown in Fig. 3 (b). When the initial states are taken in the blue point domain, the series of x is chaotic, as shown in Fig.3 (a). While the initial states are taken in the yellow point domain, the series of x is divergent, as shown in Fig.3(c). In order to increase chaotic characteristic of state x time series, the initial state of Rossler system is designed as a function of initial flight state. Furthermore, in order to produce chaotic x series, initial state can be taken only in the blue point domain. Therefore, the function of Rossler system initial state is designed as follows:

$$\begin{cases} k_{\text{sign}} = (-1)^{\Theta_0<0} \\ x_0 = k_{\text{sign}} \cdot \text{round}(\text{mod}(k_{\text{chaos}} \cdot V_0/7, 10)) \\ y_0 = -k_{\text{sign}} \cdot \text{round}(\text{mod}(k_{\text{chaos}} \cdot h_0/7, 10)) \\ z_0 = \text{round}(\text{mod}(k_{\text{chaos}}(L_0/7 + \Theta_0 \times 7), 10)) \end{cases} \tag{7}$$

where V_0, h_0, L_0 and Θ_0 are initial velocity, altitude, range and flight path angle respectively. The plus or minus sign k_{sign} is obtained from the first equation based on initial flight path angle. The function mod indicates that the first input takes the remainder of the second input, k_{chaos} denotes a scaling factor which can be used to enhance the randomness of the remainder selection. Function round indicates that the input is rounded to the nearest integer. Based on Eq.(7), x_0 and y_0 are integers in the range of $[-10, 10]$, and z_0 is integer in the range of $[0, 10]$. The initial states of the system are all located within the chaotic blue point domain, so producing chaotic series is certain.

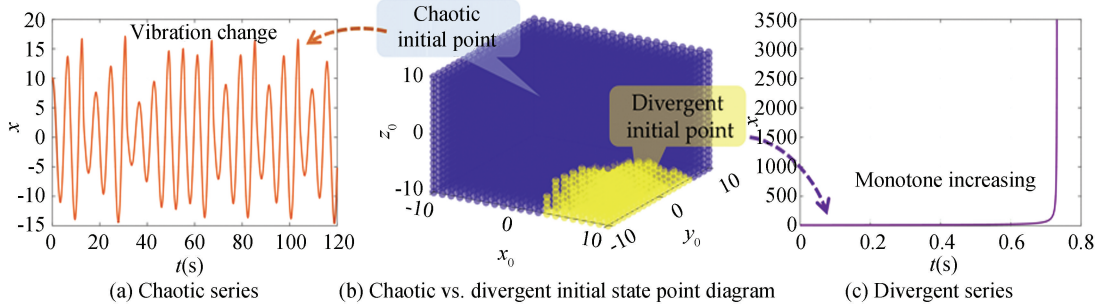

(a) Chaotic series (b) Chaotic vs. divergent initial state point diagram (c) Divergent series

Fig.3 Results of Eq.(2) with different initial conditions

3.2 Parameters Selection for Chaotic Series-based Controller

In this section, the flight trajectories with different scaling factor k_{Rossler} are simulated and analyzed based on the chaotic series-based AOA controllers. The parameter k_{chaos} is 10000, and the initial flight state is:

$$[L_0, h_0, V_0, \Theta_0] = [0\ \text{km}, 60\ \text{km}, 4.5\ \text{km/s}, 0°] \tag{8}$$

The simulations are shown in Fig. 4(a). When k_{Rossler} is 1, the change rate of AOA command is beyond the constraints specified in Eq.(5), and the AOA command oscillates between 5° and 15°, the average of AOA command is close to the maximum lift-to-drag ratio AOA, so the flight trajectories are also similar. When k_{Rossler} is 0.2, the difference in flight trajectories is not significant compared to adopting the maximum lift-to-drag ratio AOA. But the range is relatively reduced by 597.29 km, which is attributed to a severe velocity loss caused by the oscillatory change in AOA. When k_{Rossler} is 0.1, the difference in flight trajectories is the largest, due to the fact that the AOA changes gently during the pull-up process. The direction of combined force on the vehicle is continuously upward, which is beneficial to reduce velocity loss. The highest altitude of the trajectory reaches 72.53 km, where the extremely low atmospheric density results in a sharp decrease in maneuverability; the lowest altitude is 21.74 km, where the aerodynamic drag increases substantially. In order to reinforce the differences between flight trajectories, k_{Rossler} is taken as 0.1 in later sections.

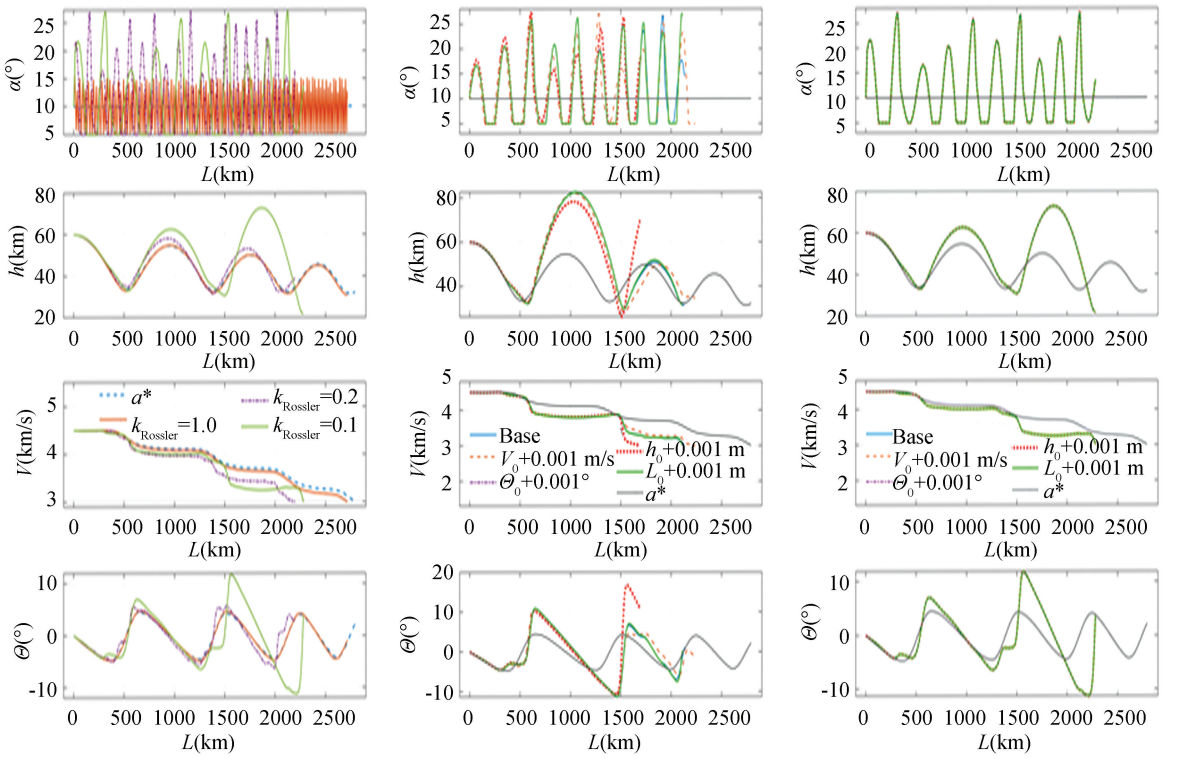

(a) Different k_{Rossler} (b) k_{chaos} is equal to 10000 (c) k_{chaos} is equal to 1000

Fig. 4 Flight simulations based on Eqs. (6) and (7)

3.3 Parameters Selection for AOA Switching Controller

In order to satisfy AOA switching control requirements as shown in Fig. 2, and take the smooth design of the switching control into account, the AOA command α_{cmd} is designed as:

$$\begin{cases} \alpha_{\text{cmd}} = \alpha_1 + \alpha_2 + \alpha_3 \\ \alpha_1 = (k_x \cdot x)\left\{\dfrac{1}{2} - \dfrac{1}{\pi}\arctan[k_{\text{ac1}}(h - H_2)]\right\} \\ \alpha_2 = \dfrac{a+b}{2} + \dfrac{a-b}{\pi}\arctan[k_{\text{ac1}}(h - H_2)] \\ \alpha_3 = A_\alpha \arctan(2\Theta)\left\{\arctan[k_{\text{ac2}}(h - H_1)] - \dfrac{\pi}{2}\right\} \end{cases} \tag{9}$$

where α_1, α_2, and α_3 are chaotic series component, constant value component, and a component for negative-feedback proportional control based on flight path angle. Parameters A_α and k_x are scaling factors, which can change the range of AOA command. The smoothing of AOA switching control at different altitude ranges is realized by inverse tangent functions. k_{ac1} and k_{ac2} can change the smoothness of the switching control with smaller values resulting in better the smoothness, H_1 and H_2 are switching signals. The AOA is a when altitude is higher than H_2, altitude gradually descends into the altitude range $[H_1, H_2]$ with low flight path angle. Angle of attack is the sum of b and $(k_x \cdot x)$ when altitude is within the range $[H_1, H_2]$. The flight simulation flow chart is shown as the solid line in Fig. 1. Parameters a and b have to satisfy the process constraints with constant AOA at different velocities, and the constraints are:

$$\begin{cases} q = 0.5\rho V^2 \leqslant q_{\max} \\ \dot{Q} = K_Q \sqrt{\rho} V^{3.15} \leqslant \dot{Q}_{\max} \\ n = \sqrt{(C_d^2 + C_l^2)}\, 0.5\rho V^2 S_{ref}/mg_0 \leqslant n_{\max} \end{cases} \tag{10}$$

where $q_{\max}$, $\dot{Q}_{\max}$, and $n_{\max}$ are allowable maximum of aerodynamic press, heating rate and load factor, respectively. Obviously, the efficient maneuvering altitude range $[H_1, H_2]$ and the constant AOA components a and b have different values at different velocities, which can be formulated as polynomial functions of velocity.

4 Simulation and Analysis

Based on the established hypersonic gliding vehicle model and the trajectory chaotification methods, the effectiveness of chaotic series-based controller and switching controller is simulated and verified.

4.1 Flight Simulation for Chaotic Series-based AOA Control

In this section, the chaotic series-based controller Eq.(6) is adopted, and the simulation analysis of flight trajectories in longitudinal channel was conducted with the initial state shown in Eq.(8).

To ensure that vehicles still have the capability to reach targets after maneuvering, the simulation stops when the velocity is lower than 3 km/s. When k_{chaos} is 10000, the flight trajectories corresponding to the presence of tiny perturbations (0.001°, 0.001 m or 0.001 m/s) in the initial state are shown in Fig. 4 (b). Due to low atmospheric density at high altitude, changes in AOA have little dynamics effect on vehicles, resulting in little difference in trajectories until the first gliding jump. In contrast, the AOA change in low altitude made noticeable differences to the trajectories.

When k_{chaos} is 1000, the same tiny perturbations of the initial state result in no effect on the trajectories, as shown in Fig. 4(c). It indicates that the chaotification of trajectories can be ontrolled by switching the parameter k_{chaos}. Eq. (7) shows that the parameter k_{chaos} determines the minimum initial flight state perturbations that can affect the initial value of the Rossler system. In addition, the altitude of the flight trajectories is too high and does not satisfy the altitude range shown in Eq. (5).

4.2 Flight Simulation for AOA Switching Control

In this section, the AOA switching controller Eq.(9) is adopted, and the simulation analysis was conducted with the initial state in Eq.(8).

When k_{chaos} is 10000, the flight trajectories corresponding to the presence of tiny perturbations (0.001°, 0.001 m or 0.001 m/s) in the initial state are shown in Fig. 5(a). Trajectory differences are strongly influenced by the change of AOA within the efficient maneuvering altitude range $[H_1, H_2]$. The perturbations of initial velocity, flight path angle, altitude and range are set to +0.001 m/s, +0.002°, +0.003 m and + 0. 004 m, respectively. The corresponding trajectories are shown in Fig. 5(b), which shows that the trajectories are obviously different right after the first gliding jump. This is due to the fact that different AOA commands are obtained from Eqs.(8), (2) and (9) based on different initial perturbations, which introduces more unpredictability to trajectories. Among the five flight trajectories obtained based on the switching controller, the maximum flight altitude is 46. 06 km and the minimum flight altitude is 35. 6 km after the first gliding jump, which satisfies the feasibility requirements shown in Eq. (5). Among them, the shortest range is 2553. 43 km, which is relatively reduced by 8. 61% compared to the range adopting maximum lift-to-drag-ratio AOA. It indicates that the introduction of chaotic trajectories has some impacts

on the range, but the introduction of stronger maneuvering characteristics at the expense of a little range is practical and acceptable. And it is feasible to reduce the impact of maneuvering on range by adjusting the efficient maneuvering altitude range, introducing AOA constraints or process constraints.

When k_{chaos} is 1000, the same tiny perturbations of the initial state result in no effect on the trajectories, as shown in Fig. 5(c).

It is also shown that the chaotification of flight trajectory can be controlled by switching the parameter k_{chaos}.

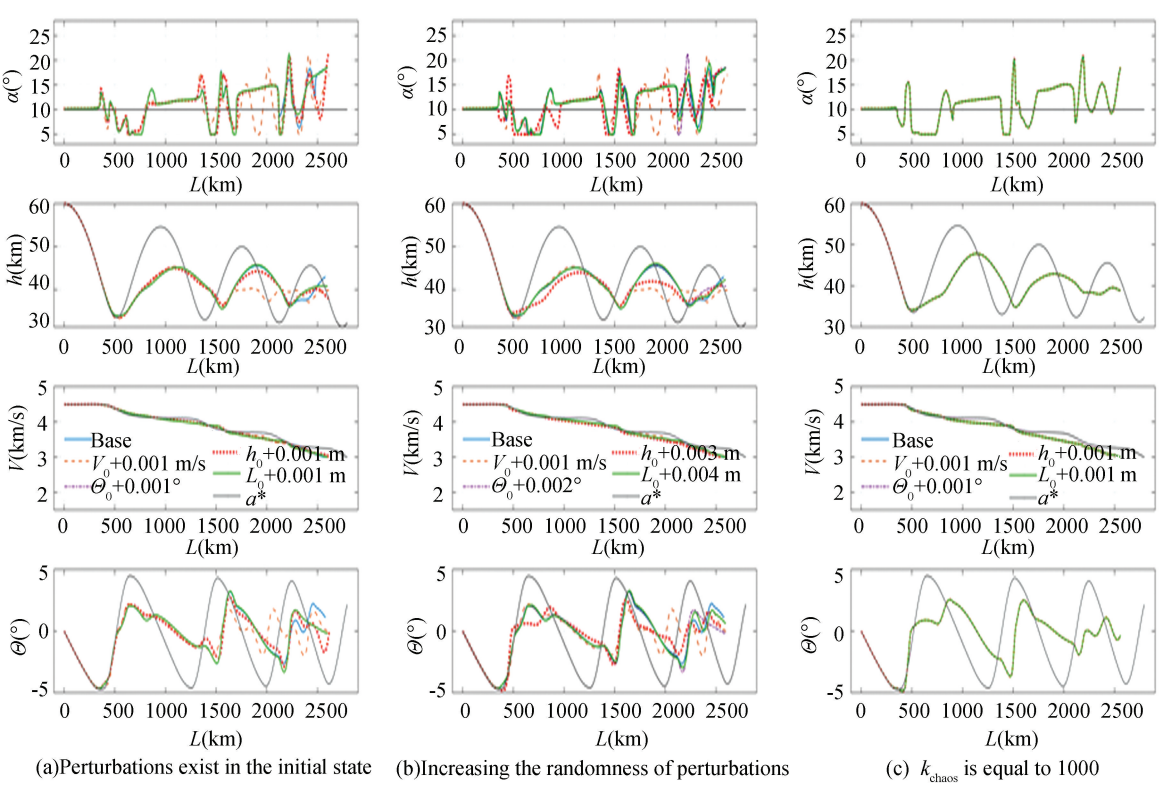

(a)Perturbations exist in the initial state (b)Increasing the randomness of perturbations (c) k_{chaos} is equal to 1000

Fig.5 Flight simulations based on Eqs. (7) and (9)

4.3 Chaotic Characteristic Analysis of Trajectories

In this section, the chaotic characteristics of the flight trajectories formed by the following four AOA control methods are analyzed:

1) The maximum lift-to-drag ratio AOA;

2) The sum of maximum lift-to-drag ratio AOA and chaotic x state time series generated by Eq.(2);

3) The chaotic series-based controller, as shown in Eq. (6);

4) The switching controller, as shown in Eq. (9).

Taking the initial state as the starting point, 50 points are selected at equal time intervals within 50 s as the initial points, and 100 points are selected at equal time intervals within 350 s as the reference points, starting from each initial points. The curve of Lyapunov exponent average value λ_{average} varying with the interval Δt is shown in Fig. 6. When using methods 3) and 4), the Lyapunov exponent is approximately 6.3 and 4.5 after the interval of 150 s, respectively. Compared with Sun et al.[13], who took function signal and chaotic series as maneuvering guidance signals, the maximum Lyapunov exponent was 0.07 and 0.56, respectively. Both methods 3) and 4) proposed in this paper can effectively increase the Lyapunov exponent and effectively improve the chaos of flight trajectory.

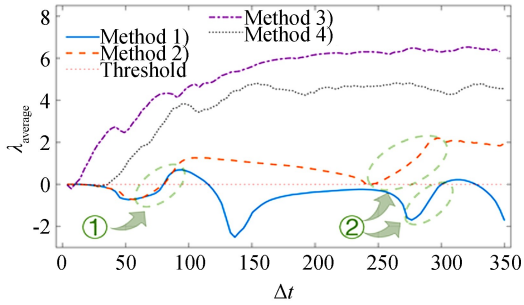

Fig. 6 Lyapunov exponent of applying various control methods

Indicating that the flight trajectories have significant chaotic characteristic. In the former case, due to the continuous change of the AOA, it shows obvious chaotic characteristic in a shorter interval. While in the latter case, a constant AOA is adopted when the flight altitude is higher than H_2, so it shows obvious chaotic characteristic after 38.5 s. In addition, the chaotic characteristic of the latter is weaker than that of the former because the latter method adopt constant AOA command at high altitude. When methods 1) and 2) are adopted, the chaotic characteristics of trajectories are significantly improved at the intervals ① and ②, which is attributed to the different AOA commands during reentry process that change the direction and magnitude of the force on vehicles, which then affects the flight state and ultimately improves the chaotic characteristics of trajectories.

Adopting methods 1) and 2), the AOA commands are certain, while the latter improves the chaotic characteristic of trajectories due to the fact that the perturbations of initial state affect the reentry state of vehicles, and both the different reentry states and different AOA commands will affect the trajectories. In contrast, the former applying a constant AOA command which has less effect on trajectories. This can be seen from elements of the Jacobi matrix corresponding to different initial state points and reference points. In the Jacobi matrix, the surfaces of partial derivatives of flight states at reference points with respect to the initial flight path angle generated by methods 1) and 2) are shown in Fig. 7(a) and Fig. 7(b) respectively. Adopting method 2) to generate the AOA command, tiny perturbations in initial flight path angle have a higher impact on the flight state at reference points. Specifically, the magnitude of the effects on velocity, flight path angle, altitude, and range at reference points, the latter being approximately four, five, six, and four times the former, respectively.

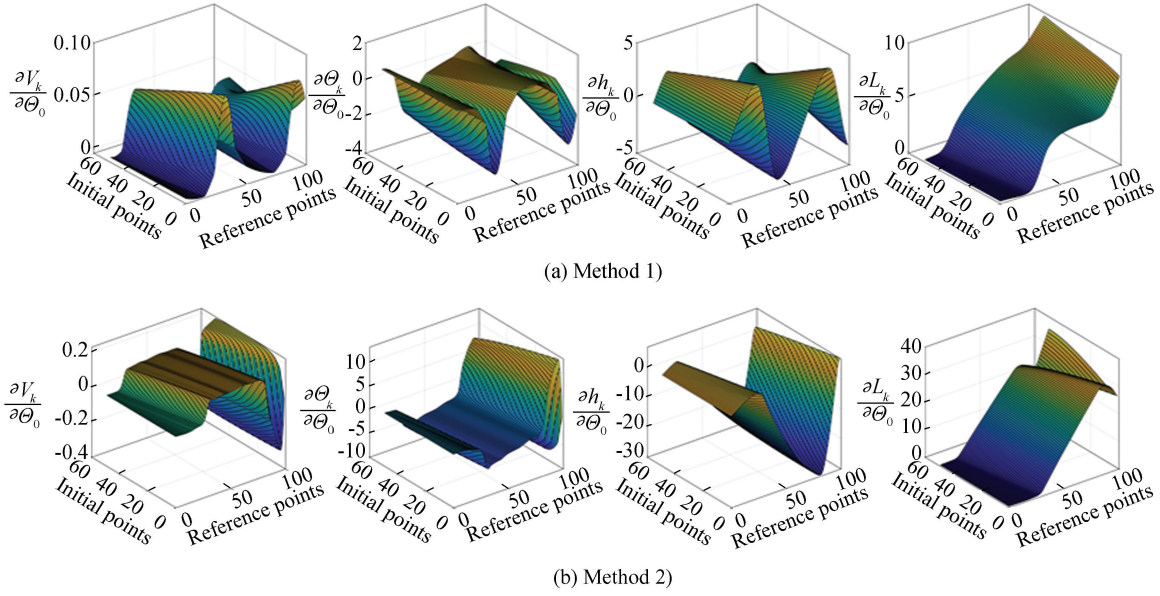

(a) Method 1)

(b) Method 2)

Fig.7 Partial derivative of flight states at reference points with respect to initial flight path angle, obtained using two AOA control methods

4.4 Stability Region Analysis of Chaotic Trajectories

In order to verify the effectiveness of the trajectory chaotification methods, this section performs a stability domain analysis of trajectories based on a conservative dynamics shown in Eq.(4), with the initial state shown in Eq. (8). Since the mechanical energy of the conservative system is constant, velocity and altitude are dependent variables, and the range is monotonically increasing, this section performs a stability region and feasibility analysis based on altitude and flight path angle two state variables.

The phase portrait starts at altitude 60 km and flight path angle 0°. The chaotic series-based controller is used to generate AOA command, and the result is shown in Fig. 8(a). The phase portrait is dispersed, and the flight path angle is close to 90° after several

gliding jumps, indicates that trajectories are not feasible. Based on the switching controller to generate the AOA command, the result is shown in Fig. 8 (b), ignoring the transition process, the range of flight path angle is 2.79° to 3.06°, and the range of altitude is 36.66 km to 50.19 km, which satisfies the feasibility requirements shown in Eq. (5).

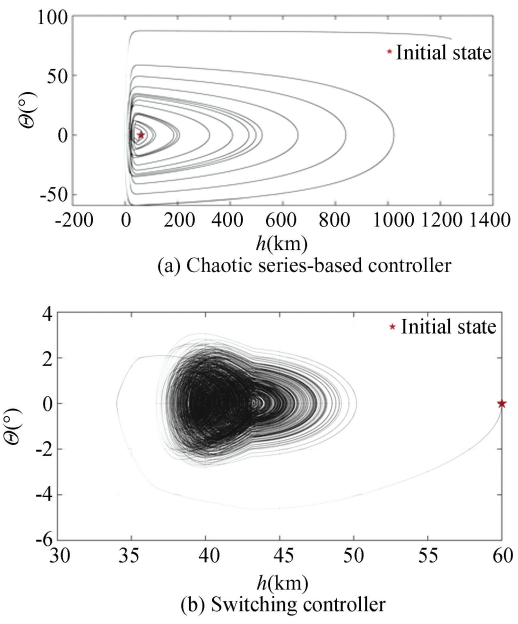

Fig. 8 Chaotic flight dynamics phase portraits

In order to analyze the stability region of trajectories with different velocities, the initial altitude is maintained, and the initial velocity is changed from 3 km/s to 4.5 km/s. The transition processes are ignored, and each 10000 s simulation process is divided into 40 time intervals. The extreme distributions of flight path angle and altitude in each interval with different initial velocity are shown in Fig. 9(a) and Fig. 9(b), respectively. The range of flight path angle is −3.48° to 3.28°, and the range of altitude is 35.19 km to 50.07 km, which meet the feasibility requirements shown in Eq.(5). The extreme values of altitude decrease gradually as the initial velocity decreases, and the extreme values of altitude are centralized at 40 km when the initial velocity is less than 3.5 km/s. It indicates that the trajectories were densely distributed between 37 km and 40 km at the end part of gliding. In this altitude range, vehicles have good maneuverability and low aerodynamic drag, with a normal overload range of 1 to 2 and a lift-to-drag ratio of 3.5.

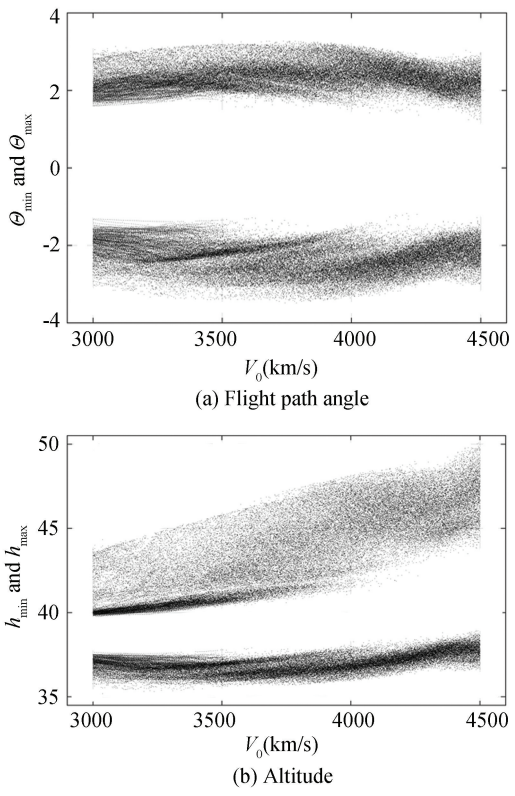

Fig. 9 Results of state variables extreme value distributions

5 Monte Carlo Flight Simulation

Since chaotic trajectories are highly sensitive to the initial state, the flight control system must have good robustness. In order to verify the robustness of the control algorithm, this section conducts a simulation through a Monte Carlo experiment to verify the feasibility of chaotic trajectories with initial state combined dispersion. In the experiment, initial state is modeled by additive perturbations[29], and the perturbation ranges are shown in Table 1. The result of two hundred Monte Carlo combined dispersion simulations is shown in Fig.10.

Table 1 Combined dispersion parameters

h_0 (km)	V_0 (km/s)	Θ_0 (°)	L_0 (km)
±3	±0.45	±2	±2

The angle of attack curves show that AOA commands of different trajectories are significantly different within the efficient maneuvering altitude range $[H_1, H_2]$, which is a key of trajectory chaotification. As the flight velocity gently decreases, the AOA commands have an overall upward trend to maintain the altitude. The minimum range is

2439.5 km, which is 12.69% less than the range adopting maximum lift-to-drag-ratio AOA. The impact of chaotic trajectories on range is limited. After the first gliding jump, the altitude range is 34.44 km to 51.2 km and the range of flight path angle is −4.14° to 3.44°, which satisfies the feasibility requirements shown in Eq.(5). Trajectory unpredictability was significantly improved after the second gliding jump. In the middle and latter part of the gliding process, the flight altitude is mainly distributed in the range of 37 km to 40 km, which is beneficial for maneuvering flight.

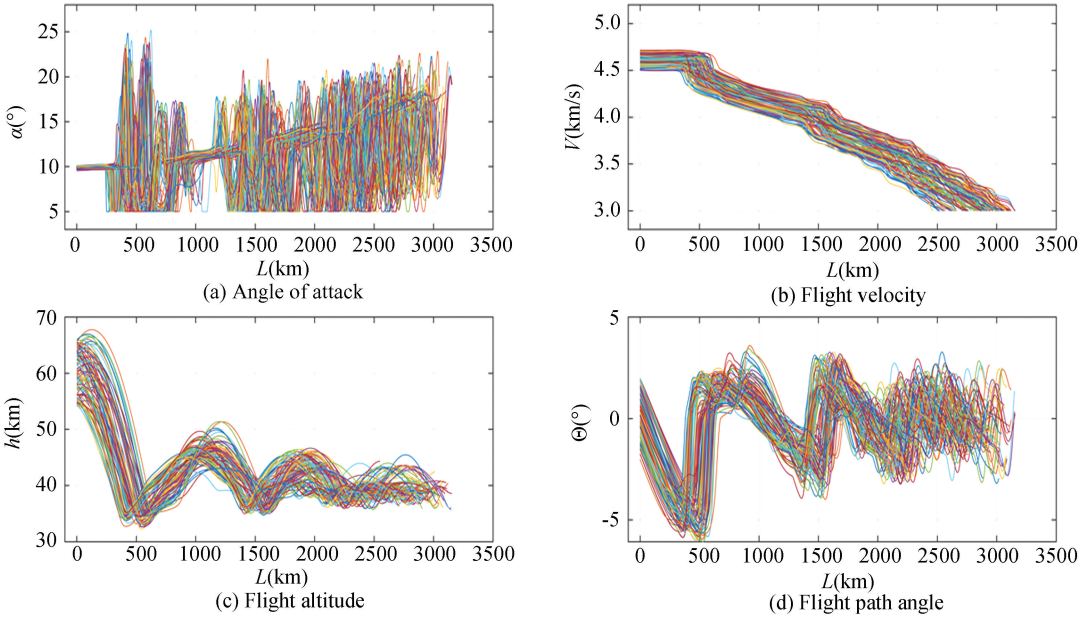

Fig.10 Monte Carlo simulation

Therefore, when there are perturbations in the initial flight state, it can be observed that the AOA switching control method considering the flight altitude designed in this study can achieve the chaotification of glide midcourse trajectory and enhance the unpredictability of trajectories. In addition, the distributions of altitude and flight path angle satisfy the feasibility requirements shown in Eq.(5) and show strong robustness.

6 Conclusions

This study primarily investigated the chaotification method for glide midcourse trajectory. As a result of our experiments, we concluded that: (1) In view of the high sensitivity of chaotic systems to the initial state, namely chaotic systems have the main characteristics of unpredictable phase portraits, a maneuvering method of hypersonic glide vehicle is proposed, which realizes chaotification of flight trajectory through chaotification of flight dynamics, and process constraints are considered. (2) This study designs a chaotic series-based AOA control method and an AOA switching control method considering flight altitude. The chaotic characteristic of trajectories is verified by continuous system Lyapunov exponent. (3) A stability region analysis method based on conservative dynamics is proposed, and the feasibility of chaotic trajectories is analyzed based on this method. Simulations show that The chaotic series-based AOA control method can realize the chaotification of trajectories, but the range of altitude and flight path angle is not feasible. And the AOA switching control method can realize chaotic and feasible flight trajectories. The latter method has strong robustness and the stability region analysis method is valuable for engineering applications.

In the future, the process constraints will be converted to AOA profile to optimize controller design. And the trajectory chaotification method in the lateral channel and 3D space will be carried out.

References

[1] Zhou W-Y, Yang D, Chen H-B. Maneuver strategy of lifting reentry vehicle. Journal of Harbin Institute of Technology(New series), 2010, 17(3): 333-337. DOI: 10.11916/j.issn.1005-9113.2010.03.008.

[2] Li G, Zhang H, Tang G. Flight-corridor analysis for hypersonic glide vehicles. Journal of Aerospace

Engineering, 2017, 30(1): 06016005. DOI: 10.1061/(ASCE)AS.1943-5525.0000667.
[3] Liu P, Liu H, Chen T, et al. Gaussian distribution-based control vector parameterization method for constrained hypersonic vehicle reentry trajectory optimization, Journal of Aerospace Engineering, 2023, 36(6): 04023075. DOI: 10.1061/JAEEEZ.ASENG-4711.
[4] Luo Y, Tan X, Wang H, et al. Trajectory prediction of hypersonic vehicles based on control quantity prediction. 2020 IEEE 4th Information Technology, Networking, Electronic and Automation Control Conference (ITNEC). Piscataway: IEEE, 2020: 87 - 91. DOI: 10.1109/ITNEC48623.2020.9084956.
[5] Hu Y, Gao C, Li J, et al. Novel trajectory prediction algorithms for hypersonic gliding vehicles based on maneuver mode on-line identification and intent inference. Measurement Science and Technology, 2021, 32(11): 115012. DOI: 10.1088/1361-6501/ac1284.
[6] Li G, Zhang H, Tang G. Maneuver characteristics analysis for hypersonic glide vehicles. Aerospace Science and Technology, 2015, 43: 321 - 328. DOI: 10.1016/j.ast.2015.03.016.
[7] Zhu J, He R, Tang G, et al. Pendulum maneuvering strategy for hypersonic glide vehicles. Aerospace Science and Technology, 2018, 78: 62 - 70. DOI: 10.1016/j.ast.2018.03.038.
[8] Zhao K, Chao D Q, Huang W H. Maneuver control of the hypersonic gliding vehicle with a scissored pair of control moment gyros. Science China Technological Sciences, 2018, 61(8): 1150 - 1160. DOI: 10.1007/s11431-017-9164-6.
[9] Hu Y, Gao C, Li J, et al. Maneuver mode analysis and parametric modeling for hypersonic glide vehicles. Aerospace Science and Technology, 2021, 19: 107166. DOI: 10.1016/j.ast.2021.107166.
[10] Yan B, Liu R, Dai P, et al. A rapid penetration trajectory optimization method for hypersonic vehicles. International Journal of Aerospace Engineering, 2019, 2019: Article ID 1490342.DOI: 10.1155/2019/1490342
[11] Shen Z, Yu J, Dong X, et al. Deep neural network-based penetration trajectory generation for hypersonic gliding vehicles encountering two interceptors. 2022 41st Chinese Control Conference (CCC). Hefei, 2022: 3392 - 3397. DOI: 10.23919/CCC55666.2022.9901735
[12] Shen Z, Yu J, Dong X, et al. Penetration trajectory optimization for the hypersonic gliding vehicle encountering two interceptors, Aerospace Science and Technology, 2022, 121: 107363. DOI: 10.1016/j.ast.2022.107363.
[13] Sun M, Yang Y, Chen Z, et al. Chaotic performance of missile's maneuvering and analysis of control ability. Control Technology of Tactical Missile, 2005(3): 8.
[14] Alsaade F W, Yao Q, Bekiros S, et al. Chaotic attitude synchronization and anti-synchronization of master-slave satellites using a robust fixed-time adaptive controller. Chaos, Solitons & Fractals, 2022, 165(part 2): 112883. DOI: 10.1016/j.chaos.2022.112883.
[15] Yadav A K. Utilizing a control technique for orbital maintenance near L_1 point and Lyapunov exponents. Chaos, Solitons & Fractals, 2024, 179: 114437. DOI: 10.1016/j.chaos.2023.114437.
[16] Molaie M, Samani F S, Zippo A, et al. Spiral bevel gears: Bifurcation and chaos analyses of pure torsional system. Chaos, Solitons & Fractals, 2023, 177: 114179. DOI: 10.1016/j.chaos.2023.114179.
[17] Darani A Y, Yengejeh Y K, Pakmanesh H, et al. Image encryption algorithm based on a new 3D chaotic system using cellular automata. Chaos, Solitons & Fractals, 2024, 179: 114396. DOI: 10.1016/j.chaos.2023.114396.
[18] Khan A, Jahanzaib L S, Trikha P. Secure communication: using parallel synchronization technique on novel fractional order chaotic system. IFAC-PapersOnLine, 2020, 53(1): 307-312. DOI: 10.1016/j.ifacol.2020.06.052.
[19] Liu X, Tong X, Wang Z, et al. A novel devaney chaotic map with uniform trajectory for color image encryption. Applied Mathematical Modelling, 2023, 120: 153-174. DOI: 10.1016/j.apm.2023.03.038.
[20] Moysis L, Lawnik M, Antoniades I P, et al. Chaotification of 1D maps by multiple remainder operator additions-application to B-spline curve encryption. Symmetry, 2023, 15(3): 726.DOI: 10.3390/sym15030726.
[21] Pisarchik A N, Jaimes-Reátegui R, Rodríguez-Flores C, et al. Secure chaotic communication based on extreme multistability, Journal of the Franklin Institute, 2021, 358(4): 2561-2575. DOI: 10.1016/j.jfranklin.2021.01.013.
[22] Şahin S, Kavur A E, Mustafov S D, et al. Spatiotemporal chaotification of delta robot mixer for homogeneous graphene nanocomposite dispersing, Robotics and Autonomous Systems, 2020, 134: 103633. DOI: 10.1016/j.robot.2020.103633.
[23] Wang Z, Ahmadi A, Tian H, et al. Lower-dimensional simple chaotic systems with spectacular features. Chaos, Solitons & Fractals, 2023, 169: 113299. DOI: 10.1016/j.chaos.2023.113299.
[24] Wang N, Cui M, Yu X, et al. Generating multi-folded hidden Chua's attractors: Two-case study. Chaos, Solitons & Fractals, 2023, 177: 114242. DOI: 10.1016/j.chaos.2023.114242.
[25] Das S, Roychowdhury S. Chaotic dynamics of off-equatorial orbits around pseudo-Newtonian compact objects with dipolar halos. Chaos, Solitons & Fractals, 2024, 179: 114410. DOI: 10.1016/j.chaos.2023.114410.
[26] Li Y, Li C, Zhong Q, et al. Coexisting hollow chaotic attractors within a steep parameter interval. Chaos, Solitons & Fractals, 2024, 179: 114406. DOI: 10.1016/j.chaos.2023.114406.
[27] Zhao H. Vehicle Reentry Dynamics and Guidance. Changsha: National University of Defense Technology Press, 1997.
[28] Liu B, Tang W. Modern Control Theory. Beijing: China Machine Press, 2006.
[29] Liu S, Lin Z, Yan B, et al. Wide-speed vehicle control considering flight-propulsion coupling constraints. Journal of Aerospace Engineering, 2023, 36(6): 04023085. DOI: 10.1061/JAEEEZ.ASENG-5066.